LA-UR- 11-05731

Approved for public release; distribution is unlimited.

Title: A Proton Radiographic Solution for Advanced Radiography at the NNSS

Author(s): N. King, D. Martinson, F. Merrill, C. Morris, G. Sinnis, M. Schulze

Intended for: Distribution to NNSA and NSTec

Los Alamos NATIONAL LABORATORY EST. 1943

Los Alamos National Laboratory, an affirmative action/equal opportunity employer, is operated by the Los Alamos National Security, LLC for the National Nuclear Security Administration of the U.S. Department of Energy under contract DE-AC52-06NA25396. By acceptance of this article, the publisher recognizes that the U.S. Government retains a nonexclusive, royalty-free license to publish or reproduce the published form of this contribution, or to allow others to do so, for U.S. Government purposes. Los Alamos National Laboratory requests that the publisher identify this article as work performed under the auspices of the U.S. Department of Energy. Los Alamos National Laboratory strongly supports academic freedom and a researcher's right to publish; as an institution, however, the Laboratory does not endorse the viewpoint of a publication or guarantee its technical correctness.

Form 836 (7/06)

A Proton Radiographic Solution for Advanced Radiography at the Nevada National Security Site

Los Alamos National Laboratory
October 2011

Authors: N. King, D. Martinson, F. Merrill, C. Morris, G. Sinnis, M. Schulze

LA-UR 11-05731 – Proton Radiography

This page intentionally left blank

Contents

Introduction....5

Technical Issues....6

Proton Radiography....7

BASE PROPOSAL : A 20-GEV PROTON SYNCHROTRON....9

OPTION: A 4-GEV PROTON SYNCHROTRON....12

Magnifying Lens System for 4-GeV System....13

Magnetic Lens System....14

Graded Approach to 20 GeV from 4 GeV....15

Resolution Scaling for Proton Radiography....17

Object Scatter Blur....18

Chromatic Aberrations....18

Detector Blur....20

Detection System and Image Analysis....21

Schedule....22

Technological Readiness and Risk Reduction....23

Cost Estimates....24

References....25

This page intentionally left blank

A Proton Radiographic Solution for Advanced Radiography at the NNSS

Introduction

The use of flash radiographic systems is increasingly critical in the development of both simulation and modeling of material behavior in high-explosive (HE)-initiated shocks. In the absence of nuclear testing, the application of flash radiographic systems is essential for the quantitative, predictive capability needed to maintain and certify the United States' nuclear weapons stockpile. Key to this effort is the implementation of radiographic capabilities that provide the necessary information for a balanced combination of integral, weapons configuration experiments and potentially less complex, focused experiments. The latter experiments could be "scaled" in the sense of requiring reduced radiographic dose (lower areal densities), but with enhanced resolution. The physics processes require the analysis of detailed material densities, velocities, and damage effects during the implosion phase of weapons systems that can best be characterized by advanced radiographic techniques in combination with velocimetry. The ultimate goal of simulations is to combine multiple, realistically modeled processes to achieve a reliable predictive capability under valid, nuclear weapons, hydro-phase conditions.

These predictions can then provide a believable simulation for comparison to the existing nuclear weapons underground testing (UGT) database. While a broad spectrum of experiments helps to validate simulations, core experiments need the highest fidelity possible to drive priorities for physics modeling. These are the HE-driven, convergent geometry, special nuclear material (SNM) experiments with weapons-relevant, pre-boost conditions. State-of-the-art radiographic capabilities should, therefore, be a very high priority and are currently not available for use with plutonium (Pu).

The increased importance of flash radiography can partly be attributed to the evolution and implementation of capabilities beyond those previously available. Newer, less familiar radiography options to the "classic" X-ray systems provide a flexible, cost-effective solution that can meet programmatic requirements. The desired and "required" capabilities have also been evolving, being broadened and driven by recent results from the performance of newer radiographic systems.

This proposal provides options that have low technical risk and high performance and that can be phased into supporting a continued scaling and surrogacy effort or be upgraded in the future. In this case, the chosen approach allows for continuing evaluation of radiographic performance and ultimately provides the capabilities necessary to validate Los Alamos National Laboratory's (LANL) hydro-phase predictive abilities for nuclear systems with the most relevance to former nuclear testing data. The result will be continued radiographic improvements for ongoing, smaller (mid-scale) experiments with SNM as well as the capability to support close to full-scale system experiments with the required effective dose, resolution, and multiple-pulse performance.

The intent is to provide a capability for SNM material-based, HE-driven radiography experimental packages. Proton radiography (pRad) capabilities will continue to improve with proton beam energy (starting with a 4-Giga-electronvolt [GeV] beam energy with the potential to upgrade to a 20-GeV beam energy) coupled with virtually the same detector system. The initial lower energy proton machine will provide the best resolution available for smaller thickness experiments in addition to a well-defined

upgrade pathway to higher energies that would deliver excellent resolution for thicker systems. Resolution blur resulting from containment constraints also improves with beam energy.

Specific applications for formulating a tested, predictive capability are contained within the current Science Campaign efforts directed towards meeting "peg-posts" within the National Boost Initiative. In particular, the implementation of the initial phase of a proton radiography capability at the Nevada National Security Site (NNSS) will improve results for LANL's 800-Mega-electronvolt (MeV), ongoing experiments at the Los Alamos Neutron Science Center (LANSCE). These can continue with minimal risk to achieving improved radiographic performance with later phase upgrades for larger systems that are relevant to subcritical experiments (SCEs). Scientists can then observe any changes in the materials physics results within a scaling format that can be tailored to isolate physics processes and to replicate the necessary weapons systems with high fidelity to ensure that pre-boost and initial conditions are met. A graded radiography approach will provide a significant resource to support Science Campaign peg-posts. This is partly due to the inherently low technical risk associated with implementation of proton radiography.

Technical Issues

Flash radiography was developed at LANL and has been evolving since 1943 for the generation of stop-action or "flash" radiographs of materials driven by high explosives for the study of dynamic material properties (such as equation-of-state, material strength, and failure modes) at high pressure, density, and strain rate [1]. The early radiographic sources utilized x-rays generated with accelerated electrons interacting with high-Z target, Bremsstrahlung sources.

Proton radiography was investigated in the early 1990s at LANL as a radiographic probe that could provide multiple-time, high-resolution radiographs of these dynamic systems [2]. By using the protons as direct radiographic probes that did not require a converter target, the limitation of a few radiographs per experiment was overcome. The major difficulty remained in overcoming the resolution limitations discovered in the very first proton radiography studies in the 1970s [3]. In these studies, high-energy protons (>100 MeV) were used as direct radiographic probes with images collected on film. From this work, it was concluded that multiple Coulomb scattering of the protons within the radiographic object resulted in significant blurring at the image, fundamentally limiting the resolution of this type of radiography. Flash radiography of dynamic systems requires the film to be located at a significant distance from the object, exacerbating the degradation in radiographic resolution by converting the angular spread of the protons into spatial spreading as they traveled from the object to the film location.

In 1995, LANL scientists discovered that this degradation of resolution could be mitigated with the introduction of a magnetic imaging lens located between the object being radiographed and the image location [4]. This lens system formed a point-to-point focus of the proton beam, removing the resolution degradation from the angular deflections within the object. This system has been used at proton radiography facilities around the world as well as in electron radiography applications[5].

With the invention of this new radiographic technique, a LANL-designed system was built to utilize the 800-MeV proton beam delivered by LANSCE [2]. This identity lens system was built from four quadrupole electromagnets with 30-centimeter (cm) apertures, providing a 120-millimeter (mm) field of view with ~180-micro-meter (µm) limiting resolution (root mean square [RMS] of a Gaussian point spread function). The proton beam at LANSCE is generated by a radio frequency accelerator, which typically delivers 12-milliampere (mA) peak proton beams for a maximum duration of 1 millisecond (ms). A deflector located at the low energy end of the accelerator can turn the proton beam on and off, providing an essentially arbitrary temporal structure. In order to take advantage of this multiple-time capability, the film of the radiography system was replaced with fast-gated, solid-state cameras (presently providing 42 radiographs per dynamic experiment). This system has been used to radiograph over 400 dynamic experiments and countless static objects.

The 800-MeV proton radiography is limited to studying objects thinner than 50 grams per square centimeters (g/cm^2) in areal density (with the requirement of >10% transmission, which corresponds to a 5-10% error on the measurement of density). In order to take full advantage of the capabilities of proton radiography, the protons must be accelerated to multi-GeV energies.

This proposal discusses two options. The first option is a cost-optimized, 20-GeV capability. In this system, a low-energy, 20-MeV linear accelerator (LINAC) injects into a booster synchrotron, which raises the proton beam energy to 500 MeV. A larger synchrotron then raises the energy to 20 GeV, providing 10 pulses of protons for each dynamic event. The second proposal is a low-energy LINAC injecting into a 4-GeV synchrotron. In the future, this 4-GeV synchrotron could act as a booster for a 20-GeV synchrotron. The 4-GeV proton beam could be used as an intermediate radiographic capability, providing four pulses of protons for each dynamic event. This option is not cost-optimized for a final 20-GeV capability, but it provides an intermediate, 4-GeV capability, meeting the immediate needs of the weapons program in a cost-effective manner.

Proton Radiography

A proton radiography facility is comprised of three primary components: the source, a contained firing site, and an imaging lens system. The proton source can either be a linear accelerator or a circular accelerator. Because a circular accelerator reuses the beam transport system in the process of acceleration, it is typically more efficient to use a circular accelerator to generate high-energy proton beams. A synchrotron accelerator is typically used for this application.

Synchrotron accelerators were developed in the 1950s for use in the study of high-energy particle physics and the technology has been extensively developed over the past 60 years. Proton synchrotrons are now "everyday items" used in applications from medical cancer treatment facilities to forefront particle searches, such as the LHC.

The beam is typically injected at relatively low energy (~200 MeV) from a linear accelerator and "stacked" into the synchrotron while the beam is circulated within the ring without acceleration. This stacking process converts the long duration of a relatively low-intensity beam current into short pulses of high current. Once the charge is transferred into the ring, an RF cavity is used to add energy to the

beam on each turn while the magnetic fields in the bending magnets are raised. As the beam is accelerated, the circulation frequency is increased along with the RF acceleration frequency until the beam has reached the design energy and is ready for extraction. Once accelerated, the beam can continue to circulate for many milliseconds until it is ready for extraction. The beam is extracted with a fast electrostatic kicker that deflects the beam into an extraction beam line, which then transports the beam to the experimental areas.

The circumference of the synchrotron is set by the field strength of the bending magnets and the final energy of the circulating proton beam. Higher energy synchrotrons require a larger circumference than lower energy synchrotrons. For very high-energy, proton acceleration (> 10 GeV), it is desirable to utilize an intermediate stage of acceleration. This intermediate stage of acceleration is called a booster ring and allows for the acceleration of more current than a single stage of acceleration. The number of pulses which can be accelerated in a synchrotron is proportional to the circumference of the ring; therefore, the number of proton pulses increases with escalating proton energy. For example, a 20-GeV proton ring can store ~10 pulses of protons while a 4-GeV synchrotron can accelerate ~4 pulses. This is simply a "real estate" argument. The proton pulses, which need to be <100 ns for flash radiography, also need to be separated by ~100 ns in order for a faster kicker to turn on between pulses. This requires 200ns per pulse. The high-energy proton beams are traveling at near the speed of light and, therefore, require ~60 m of circumference per pulse.

The imaging system is formed with quadrupole magnets. These quadrupole magnets are used to focus the proton beam similar to the way that glass lenses are used focus light beams. These magnets are then configured into a composite imaging lens which focuses protons from the object location to an image location. Figure 1 shows the trajectories of protons through an imaging lens system. A proton-to-light converter, which is typically a lutetium oxyorthosilicate (LSO) scintillator, is then viewed with fast-gated cameras. Each camera is used to collect light from each pulse of protons, allowing multiple pulse radiographs to be collected for each dynamic event. The current camera systems are capable of capturing three frames (data from three proton pulses).

The contained firing facility is composed of a spherical vessel, capable of handling dynamic loads, with blast-loaded windows that allow the protons to enter and exit the spherical vessel and vacuum beam lines for proton transport from the object to the image plane. The optimal configuration of the windows and vacuum beamlines is dependent on the energy of the proton beams. The radiographic performance of low energy protons is degraded more as they pass through containment windows than higher energy protons. A quadrupole-beam focusing system is required (after the vessel) to focus the protons that have undergone multiple Coulomb scattering. Such a magnetic lens system can be constructed to magnify the image plane, thereby increasing the spatial resolution of the system. Such an imaging system is described in more detail later in this proposal.

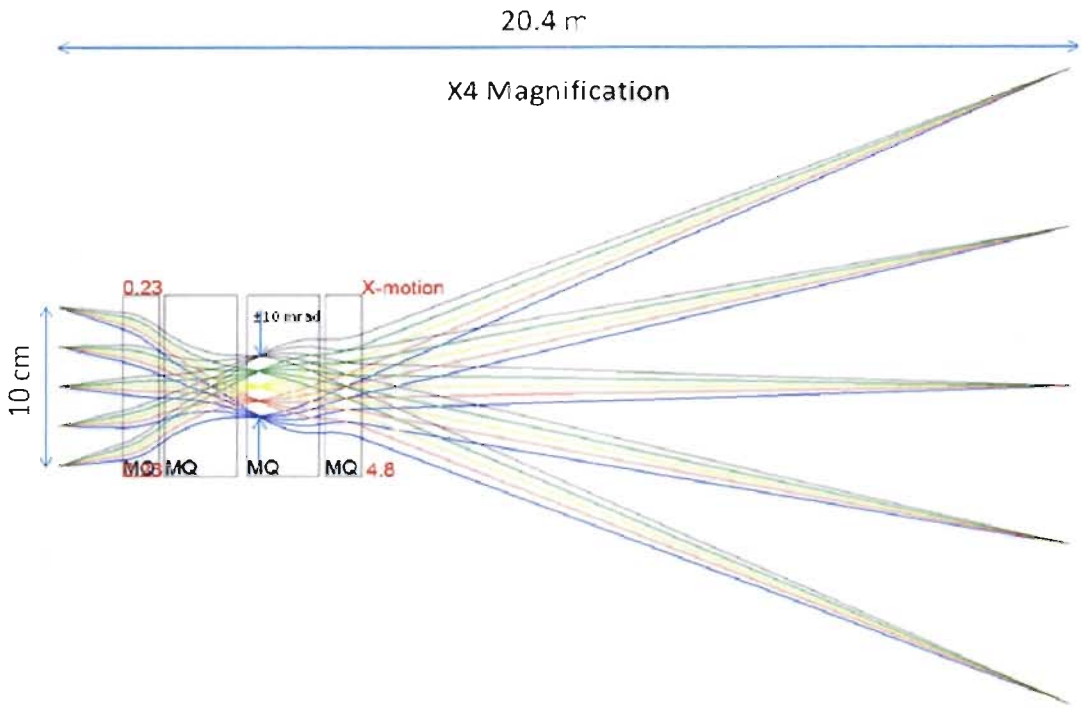

Figure 1. Proton Trajectories through a Proton Imaging Lens. *The boxes represent the region of quadrupole field while the colored lines represent the proton trajectories through the lens system. The object location is on the left, and the image location is on the right. This lens system is configured to provide a factor of X4 magnification. It should be noted that for a 100-mm diameter field of view in the object plane, the image (detector) plane will be 400 mm.*

BASE PROPOSAL : A 20-GEV PROTON SYNCHROTRON

Figure 2 shows a proposed layout for the 20-GeV proton radiography facility underground at the NNSS. This facility is composed of a negatively charged hydrogen source that is required for injection into a ring. This source is capable of injecting a 20-mA peak beam into a short LINAC, which accelerates the beam to 11 MeV and is composed of a radio frequency quadrupole (RFQ) and a drift tube LINAC (DTL). The beam is injected into a booster synchrotron, raising the beam energy to 500 MeV. Multiple proton bunches are then injected from the booster ring into the main synchrotron ring, which accelerates the beam up to 20 GeV. Once at full energy, each pulse can be independently extracted, providing radiographic images at spacing of 200 ns or larger (in multiples of 200 ns).

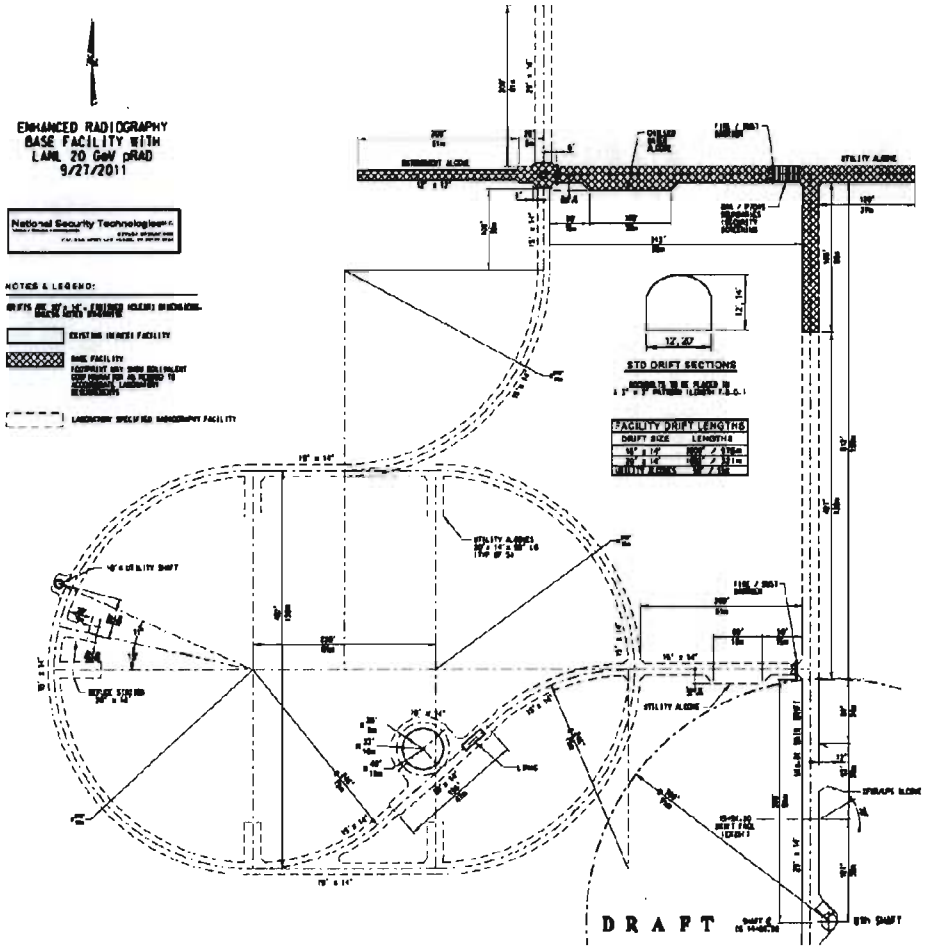

Figure 2. Facility Layout for 20-GeV Proton Synchrotron Facility Located at U1A at the NNSS. *Due to the ability to transport the proton beam, the experimental area can be well-removed from the accelerator area. In addition, the transport of the "image" protons from the object plane to the image plane isolates the detector plane to a low scatter and background region.*

The detailed design of the 20-GeV accelerator system shown in Figure 2 has been previously described in the *Design Feasibility and Cost Estimate for a Single-Axis, Multi-pulse Proton Radiography Facility* report, LA-14126 (2004). The main features of the 20-GeV synchrotron and a 500-MeV booster ring are summarized in Table 1 and Table 2. The intermediate stage accelerator provided the most cost-effective solution for a full-energy, 20-GeV, proton machine. The desire for a "graded" approach to the full-energy machine and an intermediate proton energy radiographic capability is driving consideration for a multi-pulse, 4-GeV booster described in the following text.

Table 1. Parameters for 20-GeV Synchrotron Lattice

Circumference	608 meters
Number of Dipole Magnets	56
Dipole Length	5.0 meters
Dipole Field	1.56 Tesla
Dipole Gap	5 cm
Number of Quadrupole Magnets	76
Quadrupole Length	0.8 meters
Quadrupole Gradient	11.3 Tesla/meter
Quadrupole Aperture	10 cm
Transition Gamma	5.73
Admittance (normalized)	16 π mm-milliradians (mr)

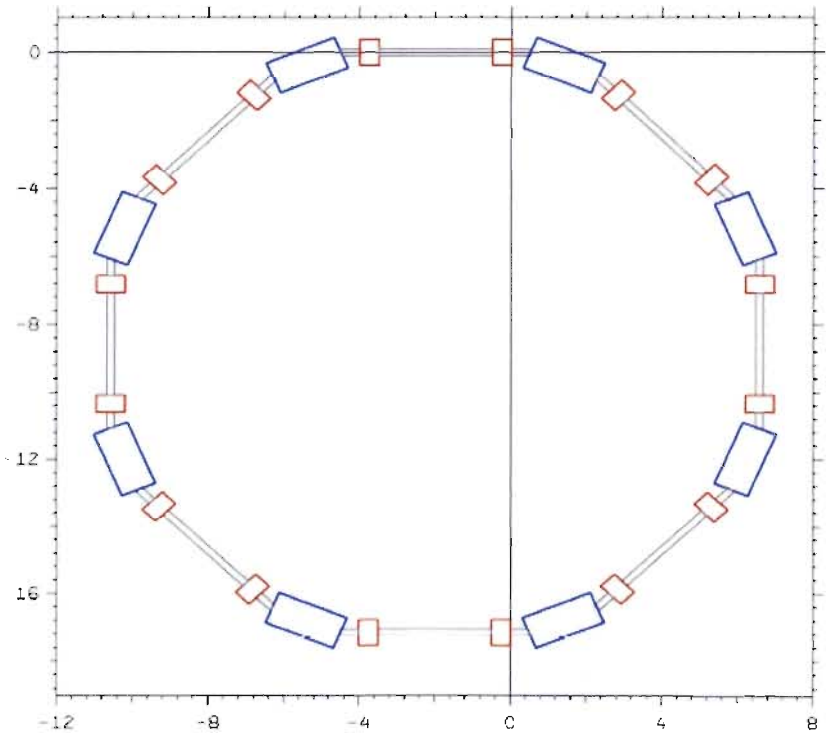

Figure 3. 500-MeV Booster Layout

Table 2. 500-MeV Booster Parameters

Circumference	56 meters
Number of Dipole Magnets	8
Dipole Length	2.0 meters
Dipole Field	14.3 k Gauss
Dipole Gap	10 cm
Number of Quadrupole Magnets	16
Quadrupole Length	0.5 meters
Quadrupole Gradient	3.5 Tesla/meter
Quadrupole Aperture	15 cm
Transition Gamma	2.3
Admittance (normalized)	34 π mm-mr

OPTION: A 4-GEV PROTON SYNCHROTRON

The 4-GeV synchrotron considered in this proposal was designed as a booster accelerator for the Advanced Hadron Facility (AHF) 50-GeV ring [5]. This synchrotron is a symmetric, nine-sided lattice with a circumference of 261 m. This synchrotron was designed to be operated at 5 Hz, a bit higher repetition rate than is required for NNSS activities. The injection energy was assumed to be 157 MeV, the output energy of the existing RFQ/DTL/CCL (cavity-coupled LINAC) linear accelerator at the spallation neutron source (SNS) at Oak Ridge. This accelerator system is approximately 3/35/40 meters respectively for a total required length of ~100 m. Although, this LINAC was designed for a high-duty factor, and the design for this system would be for lower duty, the length of this LINAC system provides a reasonable estimate of the facility requirements for LINAC injection into a 4-GeV synchrotron.

At 4 GeV, the revolution frequency of the ring is 1.13 μs with a period of 885 ns. The design considered for the AHF booster option was an h=1 system, which means that only a single bunch was accumulated with a total charge of 4×10^{12} protons. With the assumption that this single bunch would be reconfigured into four bunches, each 100-ns long with a separation of 100 ns, this ring is capable of delivering four pulses, independently timed, each pulse containing 1×10^{12} protons. This can then utilize the same firing site and detector system as the 20-GeV option.

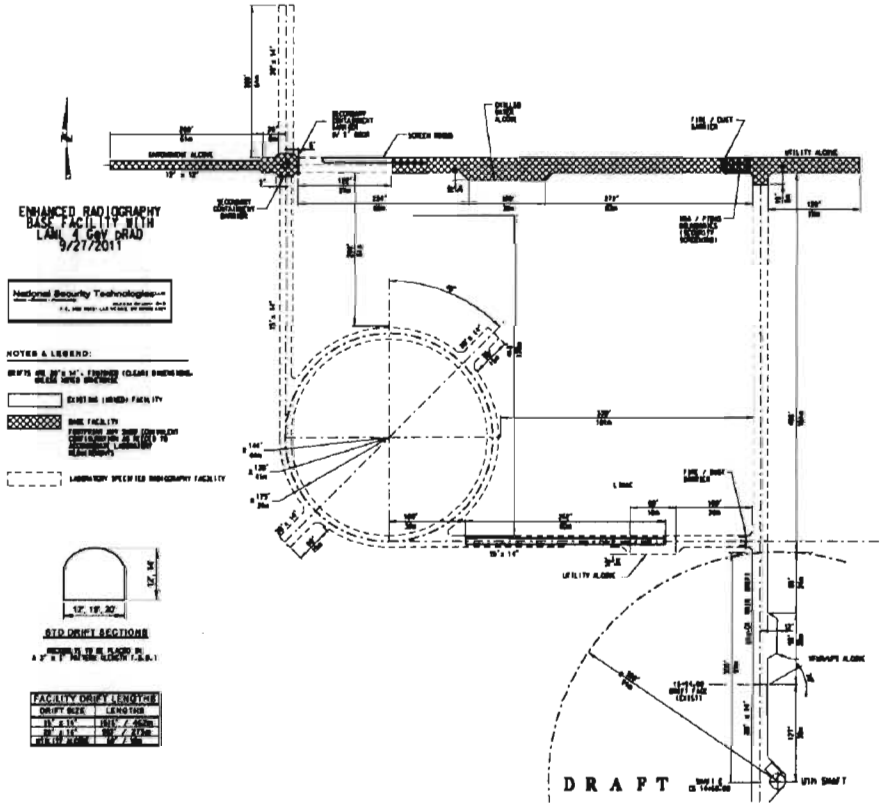

Figure 4. Facility Layout for 4-Gev Proton Synchrotron Facility Located at U1A at the NNSS

In the following text, the magnifying lens system and the lens imaging system for the 4-GeV option are described.

Magnifying Lens System for 4-GeV System

A conceptual design has been developed for the 4-GeV imaging system. This system is assumed to be built from conventional electromagnets having pole-tip fields of 1.2 Tesla. The first magnet would be located 1.3 m downstream of the object location in order to accommodate a 6-foot vessel. In order to achieve a 10 x 10-cm field of view, the magnet apertures were chosen to be 2-cm (9 inches) diameter. With this configuration, particle tracking codes were used to design a X4 magnifying lens capable of focusing 4-GeV particles. The length of the quadrupoles must be 0.75 and 1.5-m long in order to minimize the chromatic aberration of the lens system. Also with this configuration, the physical length of the imaging system is 20.5 m with a chromatic length of 9.4 and 5.6 m in the horizontal and vertical directions. Figure 5 shows the proton trajectories through the imaging lens.

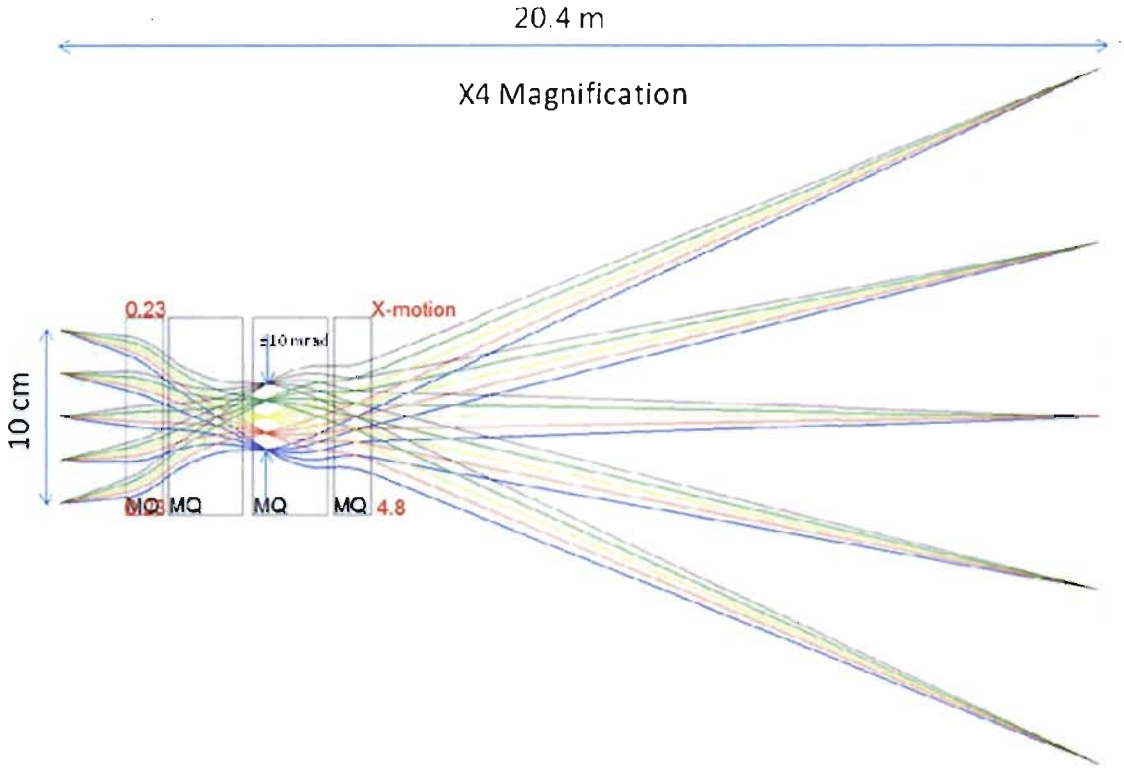

Figure 5. Proton Trajectories through a X4 Magnifying Lens Designed to Focus 4-GeV Protons. *The lens system is 20.5-m long with a chromatic length of 9 m. The field of view of the system is 10 x 10-cm with an angular acceptance of ±10 mrad. Note that the same number of protons per pulse can be redistributed into a smaller field of view (FOV), depending on experiment specifics.*

Magnetic Lens System

A conceptual design has been developed for the 4-GeV radiographic imaging system. This system is assumed to be built from conventional electromagnets having pole-tip fields of 1.2 Tesla. The first magnet would be located 1.3 m downstream of the object location in order to accommodate a 6-foot vessel. In order to achieve a 10 x 10-cm field of view, the magnet apertures were chosen to be 30.5-cm (12 inches) diameter. With this configuration, particle tracking codes were used to design an identity lens capable of focusing 4-GeV particles. The length of the quadrupoles must be 1.5-m long in order to minimize the chromatic aberration of the lens system. With this configuration, the physical length of the imaging system is 11.5 m with a chromatic length of 13.5 m. Figure 6 illustrates the proton trajectories through the imaging lens.

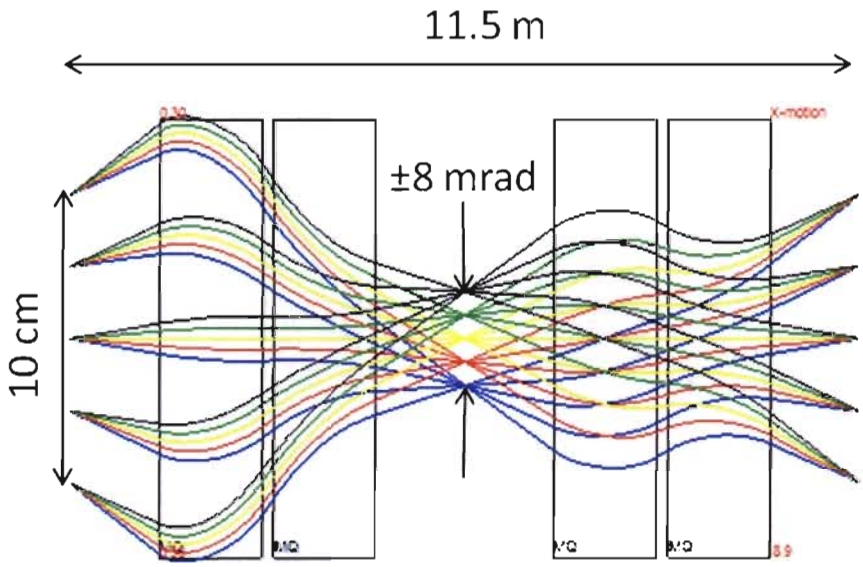

Figure 6. Proton Trajectories through an Identity Lens Designed to focus 4 GeV protons. *The lens system is 11.5-m long with a chromatic length of 13.5 m. The field of view of the system has a maximum of 10 x 10 cm^2 with an angular acceptance of ±8 mrad.*

This system has a ±8-millirad (mrad) angular acceptance over the full 10-cm field of view. The matching condition, which is required to partially cancel chromatic aberrations, is Mx=-0.29 m^{-1} and My=0.29 m^{-1}.

Graded Approach to 20 GeV from 4 GeV

For completeness, LANL proposes a U1A option for first implementing a 4-GeV option with significant improvements over the current Cygnus x-ray radiographic capability (Figure 7). This option can readily be upgraded to the full 20-GeV capability with a 4-GeV booster (Figure 8) to provide enhanced, multi-pulse capability coupled with improved resolution and larger areal density options. The enhanced resolution is derived primarily from the smaller contributions due to containment of higher HE experiments.

The importance of the "graded approach" cannot be overemphasized. The initial phases of 4 GeV shift the cost profile decidedly towards implementation of the firing site and U1A infrastructure costs needed for any radiographic capability. The initial radiographic, 4 GeV option then provides a significant enhancement to potential radiographic capabilities for smaller scale experiments with multi-pulse [4] and resolution exceeding current requirements with well-established accelerator technology (low risk). It also provides the basis for remaining internationally competitive in flash radiography to permit U.S. requirements to evolve and grow to a full, higher areal density capability. This enhancement to the complex can then be implemented with relatively modest costs to the 20-GeV option.

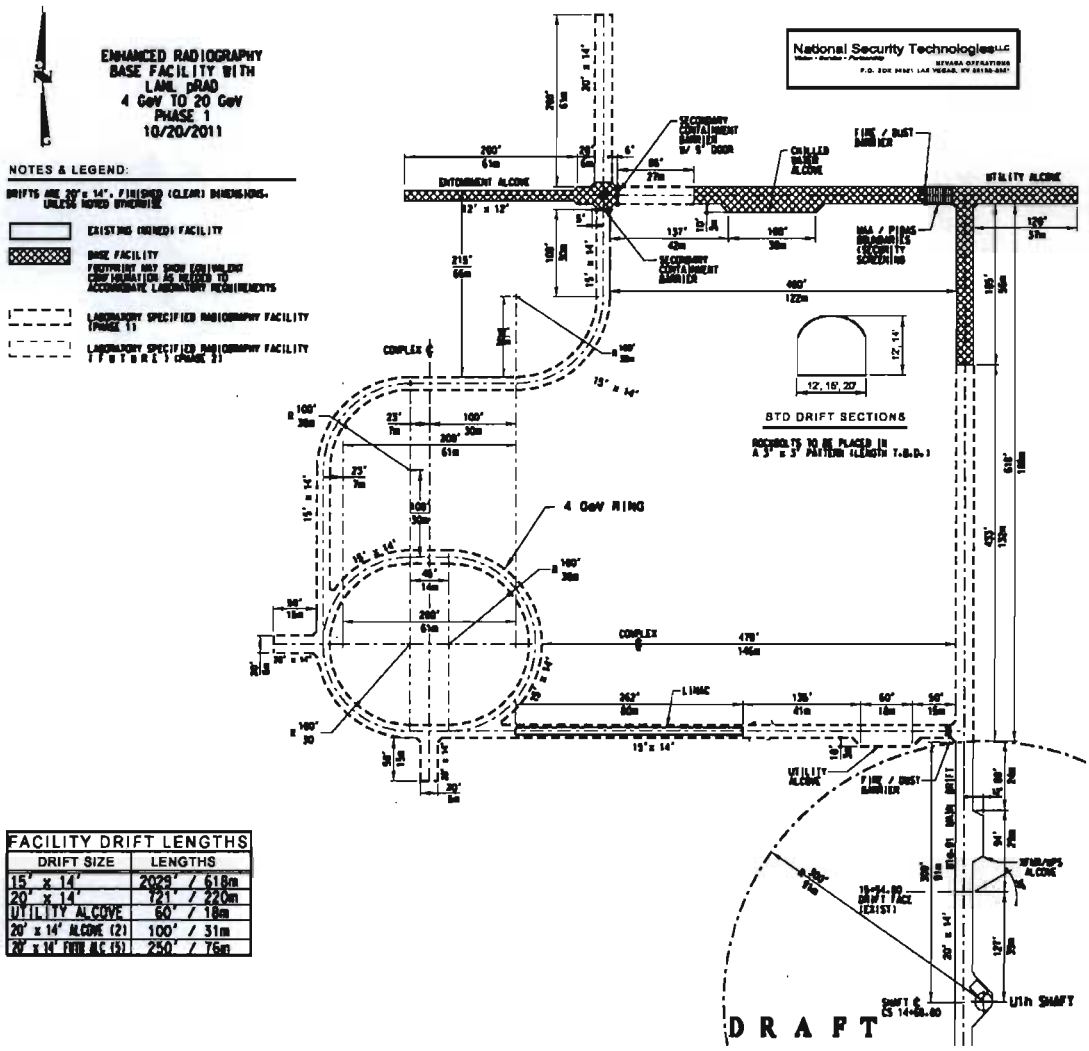

Figure 7: Alternative Implementation of a 4-GeV Option into the Proposed NNSS/U1A Firing Site Configuration. *This layout is compatible with the future implementation of a 20-GeV enhancement to full, proton radiographic capabilities utilizing the U1A firing site and infrastructure capabilities depicted in Figure 7.*

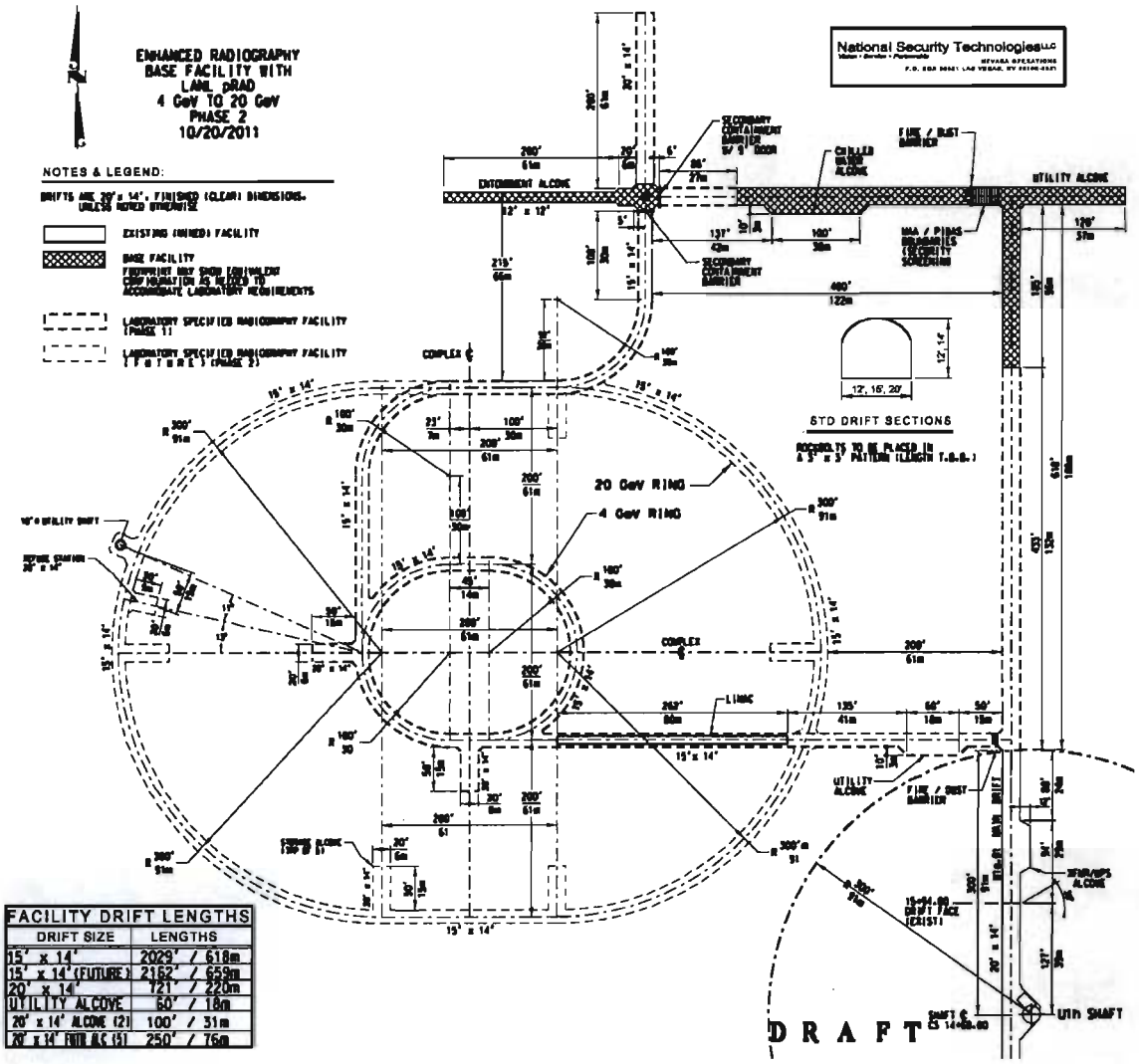

Figure 8: Alternative Implementation of a 4 GeV Option Into the Proposed NNSS/U1A Firing Site Configuration. *This layout is compatible with a previously implemented 4 GeV radiographic capability utilizing the already existing U1A firing site and infrastructure capabilities shown.*

Resolution Scaling for Proton Radiography

Unlike radiographic systems based on x-rays, the concept of a spot size for the beam is not relevant in understanding the limiting resolution of a proton radiographic facility. In addition, the radiographic "image" can be transported as a proton spatial distribution, much as a visible image can be transported by a visible lens system. As a result, there are three main contributors to the resolution of a proton radiography system:

1. Object scattering: introduced as the protons are scattered while traversing the object
2. Chromatic aberrations: introduced as the protons pass through the magnetic lens imaging system
3. Detector blur: introduced as the proton interacts with the proton-to-light converter, and the resultant visible light image is lens-relayed, gated, and collected with a camera system

Object Scatter Blur

Protons undergo multiple Coulomb scattering as they traverse an object, resulting in small deflections of the proton trajectories. After leaving the object, the proton is focused by the magnetic lens to form an image, and this deflection results in blur at the image location. This process is shown in Figure 9. The incident proton passes through the object to the point of interest, typically a region in the center of the object. Scattering upstream of the point of interest does not result in significant contribution to the blur function. Scattering downstream of the object, however, results in a small position offset and a small angular deflection, which results in a small error in the position of the proton at the image location. Because multiple Coulomb-scattering results in nearly a Gaussian distribution of scatter angles, the resulting point-spread function is very close to a Gaussian distribution. The RMS width of the resulting blur function can be calculated with Equation 1 that indicates this source of blur scales inversely with incident proton momentum. Resolution improves as the incident proton momentum increases.

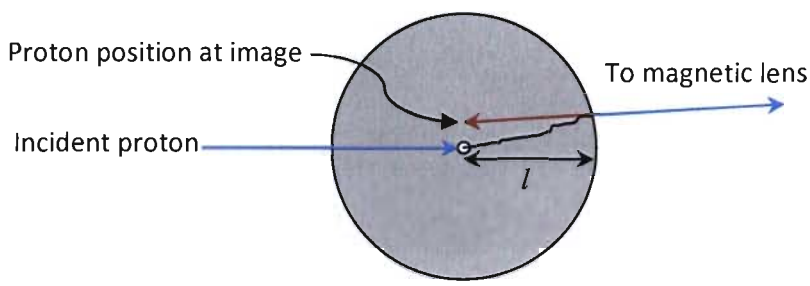

Figure 9: Object Scatter Blur Results from Small-Angle Scattering within the Object, Downstream of the Point Of Interest. *The small angular deflection results in a small position error at the image location as the proton is focused by the magnetic lens system.*

Equation 1:

$$\sigma_o = \frac{1}{\sqrt{3}}\theta\frac{l}{2} = \frac{14.1}{\sqrt{3}}\frac{1}{p\beta}\sqrt{\frac{l^3}{x_o}} \propto \frac{l^{\frac{3}{2}}}{p}$$

Equation 1: Relationship Between the RMS Blur (σ_o) of a Gaussian Point-Spread Function and the Object Thickness, Downstream of the Point Of Interest (*l*) and the Scattering Angle of the Proton, Downstream of the Point Of Interest ($\theta = 14.1/P\beta\ \sqrt{(l/x_o)}$). *In this equation, p is the proton momentum; β is the relativistic velocity; and x_o is the radiation length for the object material.*

Chromatic Aberrations

Chromatic aberrations, which also contribute to image resolution, are a result of off-momentum protons being focused differently by the magnetic imaging lens system. The magnetic lens is set to focus protons of one momentum. Off-momentum protons are not focused perfectly, resulting in image blur. The relationship of the RMS blur (σ_c), which is typically a Gaussian point-spread function, to the

scattering angle,θ, the fractional momentum offset (δP/P), and the chromatic length of the lens system (l_c) is shown in Equation 2 and ray traces with three energies (momenta) in Figure 10.

Calculations show that for a conventional (non-superconducting), non-magnifying, magnetic lens system with pole-tip fields of ~1T and a field of view of ~100 mm, the chromatic length of the lens system grows as the square root of the proton momentum. This is shown in Figure 11. With these assumptions, the chromatic resolution for relativistic protons scales inversely with momentum to the three-half-power.

Equation 2:

$$\sigma_c = l_c\theta\frac{\delta P}{P} = c\sqrt{P}\frac{\delta P}{P^2}\frac{14.1}{\beta}\sqrt{\frac{l}{x_o}} \propto \sqrt{\frac{l}{P^3}}$$

Equation 2: Relationship Between the Resolution Due to Chromatic Aberrations and the Object Thickness and Momentum of the Proton Beam

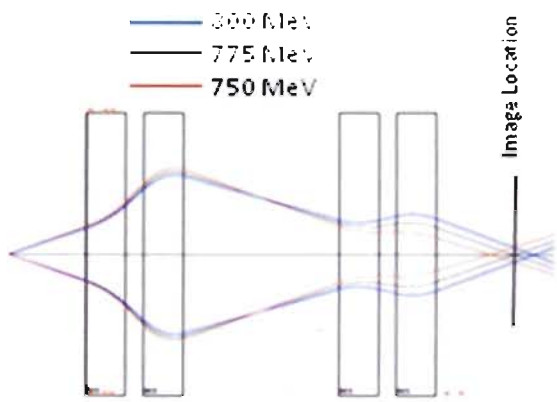

Figure 10. Proton Trajectories through an Identity Lens Demonstrating the Source of Blur Due to Chromatic Aberrations. *Low-energy protons are focused upstream of the image location while higher energy protons are focused downstream of the image location.*

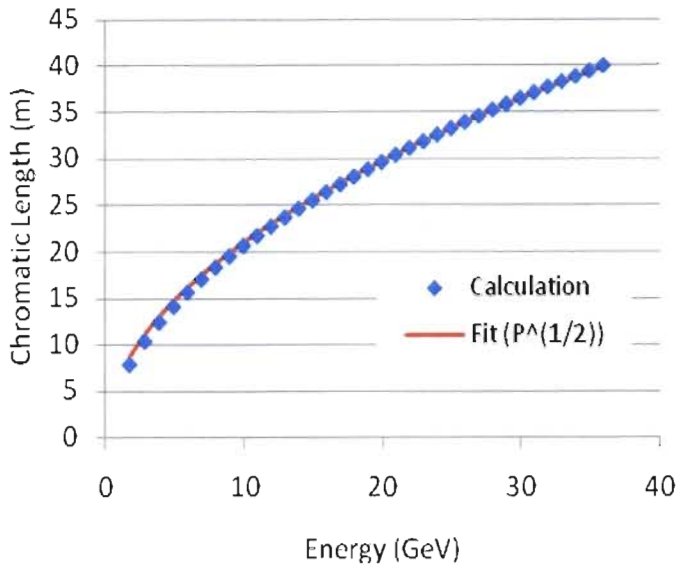

Figure 11. The Chromatic Length of a Conventional Imaging Lens System. *This lens system, with ~1-T pole tip field, was calculated for systems with ~100-mm field of view for various proton energies. The chromatic length increases as the square-root of the proton momentum.*

Detector Blur

The resolution from the proton-to-light converter is set by the proton-to-light conversion mechanism, the thickness of the converter medium, and the angular spread of the proton beam passing through the converter. As the proton energy increases, the angular deflections are reduced, resulting in smaller blur contributions to the radiography system. Equation 3 shows how this contribution to blur contributes to the radiographic resolution of the system. As the proton energy increase, the angular spread of the proton beam due to multiple Coulomb scattering, which is assumed to be the dominant source of angular spread in Equation 3, will be overcome by small-angle nuclear elastic scattering. As nuclear interactions dominate the angular spread, they will have significantly more complicated and material-dependent angular distributions (not considered here).

Equation 3:

$$\sigma_s = \theta l_s = l_s \frac{14.1}{P\beta}\sqrt{\frac{l}{x_o}} \propto l_s \sqrt{\frac{l}{P}}$$

Equation 3: Relationship Between the Resolution Due to Proton-to-Light conversion, the Object Thickness, Converter Thickness, and Momentum of the Proton Beam

The imaging camera's contribution to the radiographic resolution should be independent of momentum and object thickness. Present technologies deployed for 800-MeV proton radiography typically have up

to ~1000x1000=10^6 pixels that fix the relationship between field of view and resolution. This pixel count is not a fundamental limit, but is available within existing camera systems and is adequate for current, smaller-scale experiments. Some detector development would be needed to better match the achievable magnetic lens, the radiation-to-light converter resolution, and the resolution contribution of the visible imaging detector component to improve the system radiographic resolution. The detector development needed does not depend on developing a new technology, but rather on optimizing an existing capability to larger numbers of pixels.

Detection System and Image Analysis

The detection system currently used at the LANSCE Proton Radiography Facility can be modified to capture images for the systems proposed in this document. However, to take full advantage of the improved resolution of these systems and the increased size of objects under study, new imaging sensors are currently under development. These new sensors are based on complementary metal oxide semiconductor (CMOS) readout technology (i.e., the current camera system); however, they will have larger numbers of pixels, lower noise level, more frames, and faster interframe times and shutter speeds. Table 3 gives the capabilities of the current camera system and the systems currently being developed in collaboration with Teledyne and NSTec.

The Technical Readiness Level (TRL) of these new cameras is rated as 2-3, and work is ongoing to complete this development over the next few years. The 10-frame option is targeting the existing multi-pulse, LANSCE proton capability while the two-frame option with higher pixel number will target a broader range of applications. These include: LANSCE (pRad), Cygnus U1A x-ray radiography enhancements, and the National Ignition Facility (NIF) neutron imaging requiring high detector quantum efficiency(DQE)-gated imagers as well the needed higher resolution option for a 4-GeV proton, four-pulse option, and risk mitigation for the Dual Axis Radiographic Hydrodynamic Test facility (DAHRT-II). The two-frame option is also somewhat simpler and will provide good risk mitigation for the more complex, 10-frame option needed for the LANSCE pRad facility.

Table 3. Comparison of Current Generation, Hybrid, CMOS Camera System to Systems under Development in Collaboration with Teledyne and NSTec.

Current Hybrid CMOS Camera	New Hybrid CMOS Cameras (Prad2 / HiRes1)
3 frames	10 frames/2 frames
720x720 pixels	1024x1024 pixels/2000x2000 pixels
11.4 bit dynamic range (~ 150e noise floor)	12 bit dynamic range (≤ 50e noise floor)
> 150ns integration time	~ 50ns integration time/< 50ns integration time
26 micron pixels	40 micron pixels/23 micron pixels

The image analysis software currently used by the LANSCE Proton Radiography Team was written specifically for LANSCE (pRad) and (U1A/NNSS x-ray) radiography. While it is fast, robust, and provides excellent density reconstructions and spatially calibrated radiographs, LANL proposes to provide increased flexibility, incorporating the Bayesian Inference Engine (BIE) tool currently used by the international flash x-ray community (including DARHT) into the proton radiographic "tool box." The BIE teams at LANL and the Atomic Weapons Establishment (AWE) are now working to incorporate proton radiography physics into this methodology.

An important component of a proton LINAC is the reproducibility of the beam. The pulse-to-pulse intensity variation is presently measured and utilized in the calibration for all experiments. For each experiment, a beam current monitor is used to measure the beam intensity, and calibration objects are placed in the field of view along with the experiment so that pulse-to-pulse variation in beam intensity can be measured and corrected in the final analysis of the experiment.

Schedule

The schedules for the 20-GeV and 4GeV proton radiographic facilities are shown in Figures 12 and 13. Note that these are integrated schedules that include NNSS design and mining efforts.

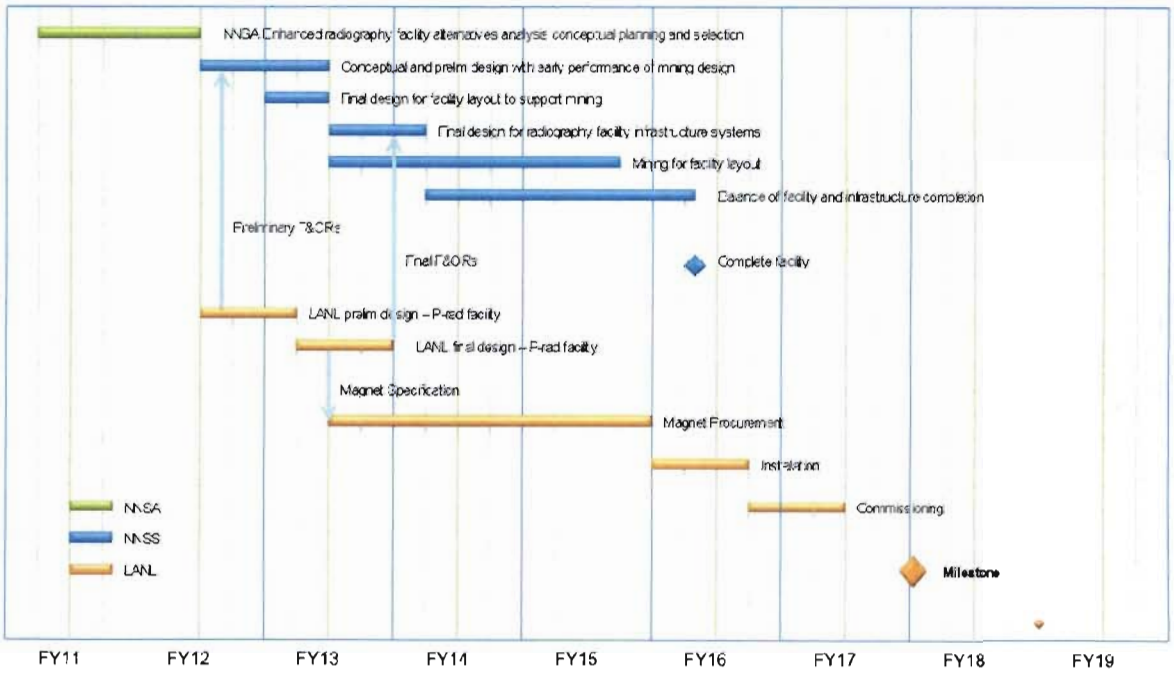

Figure 12. Schedule for Design and Construction of a 20-GeV Proton Radiographic Facility at U1a

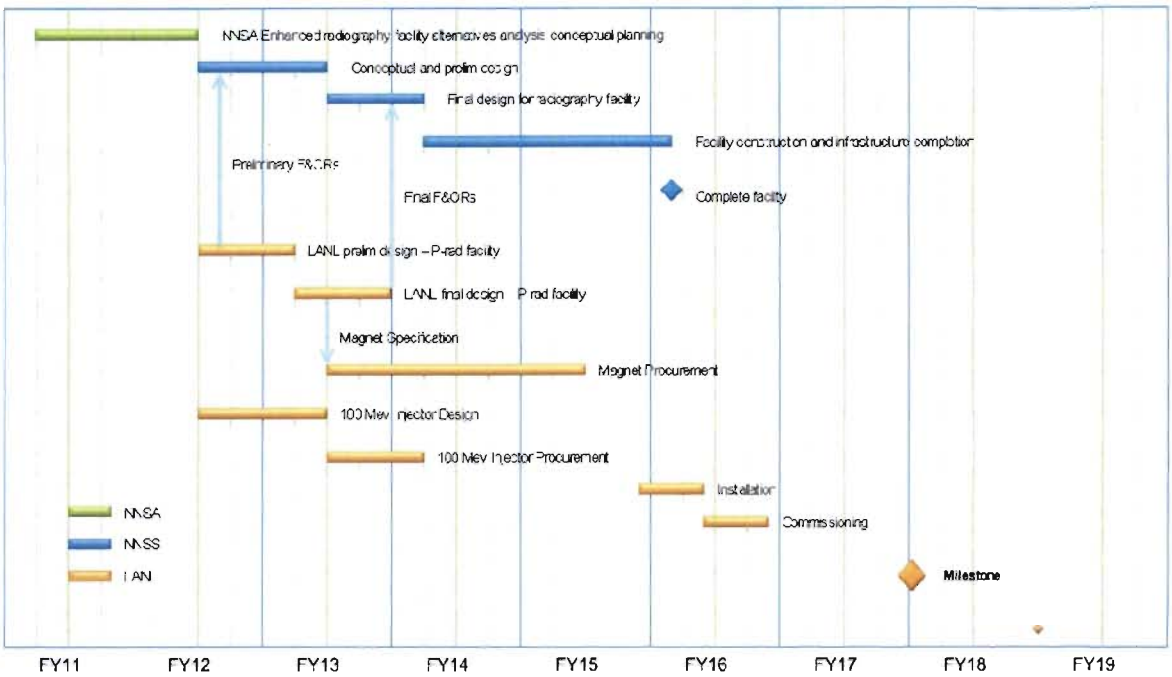

Figure 13. Schedule for Design and Construction of a 4-GeV Proton Radiographic Facility at U1a

Technological Readiness and Risk Reduction

Both proposed proton radiographic systems (20-GeV and 4-GeV proton synchrotrons) have a TRL of 9 and have a low technological risk. As previously discussed, proton synchrotrons are now commonly in use. The highest energy system now exists at the CERN facility in Switzerland and is capable of accelerating protons to ~10 Teraelectronvolt (TeV, i.e., the Large Hadron Collider). At the Fermi National Accelerator Laboratory in Batavia, Illinois, a proton synchrotron accelerating and colliding 1-TeV protons has been operational since the 1990s (and is now being decommissioned). Brookhaven National Laboratory has built and is operating a 24-GeV synchrotron (the Alternating Gradient Synchrotron). LANL has previously carried out a series of static experiments at Brookhaven, and future collaboration with them would be fruitful for this proposal.

Proton LINACs are also quite common (TRL 8-9). The 800-MeV LINAC at LANL has been operating since the 1970s, and a high-power, 1-GeV LINAC at the SNS at Oakridge National Laboratory has been operating since 2005. In addition, there are many commercial, low-energy (<~30 MeV) LINACs available that are in use in numerous hospitals and research facilities throughout the country. Based on this history, LANL believes that the TRL of either option presented in this proposal is between 7 and 8.

Because of the long history of LANSCE (and the Los Alamos Meson Physics Facility) at Los Alamos, there is significant expertise in LINAC design, construction, maintenance, and operation. LANL expects to partner with either Brookhaven or the Fermi Lab for assistance with the design and construction of the proton synchrotron.

While the technological risk of this proposal is quite low, the detailed design of either option should begin as soon as possible. To obtain four pulses, a fast kicker must be developed. Such a fast kicker could be based upon current LANL pulser design, which has demonstrated 15 pulses over a 1.6-microsecond period. Preliminary design work to develop this kicker for 50-GeV protons has already occurred in the context of the AHF proposal. For a 4-GeV proton synchrotron, the demands are significantly lower. We estimate the TRL of this fast kicker system to be between 5 and 6. Because a two-pulse system will meet the current requirements, this does not impact the overall TRL of the project. Also a 4X magnification system (while not yet built) is quite similar to the 3X magnifier now in operation at the LANSCE pRad facility and does not represent a technological risk (TRL 7). Rough cost estimates are given in Table 4.

Cost Estimates

Table 4. Cost Projections ($Millions). Basis for FY2011 Cost

Device	Source/Driver	Detectors	Installation & Commissioning	System Design & Engineering	Other Costs	Total – Device Only
pRad 20 GeV	$68-99	$4-7	$35-50	$13-18	$83-120	$202-293
pRad 4 GeV	$37-55	$4-7	$24-34	$10-15	$53-77	$128-186

Cost notes:

- Source and Driver - equipment costs only
- Detection System - equipment costs only
- Installation and Commissioning - LANL costs associated with installation, connection to utilities and machine commissioning
- System Design and Engineering - LANL costs associated with engineering design for machine and facility integration
- Other Costs - includes G&A, assuming programmatic operating dollars (not line item) + 6.75%
- NM Tax amounts are applied to items above.
- Does not assume escalation, contingency, formal project management, QA, or facility start-up costs.

References

[1]G. S. Cunningham, C. L. Morris, "The Development of Flash Radiography", Los Alamos Science, 28, 76-91, 2003.

[2] N. S. P. King, E. Ables, K. Adams, K. R. Alrick, J. Aman, S. Balzar, P. D. Barnes, M. L. Crow, S. B. Cushing, J. C. Eddlemann, T. T. Fife, P. Flores, D. Fujino, R. A. Gallegos, N. T. Gray, E. T. Hartouni, G. E. Hogan, V. H. Holmes, S. A. Jaramillo, J. N. Knudson, R. K. London, R. R. Lopez, T. E. McDonald, J. B. McClelland, F. E. Merrill, K. B. Morley, C. L. Morris, F. J. Naivar, E. L. Parker, H. S. Park, P. D. Pazuchanics, C. Pallai, C. M. Riedel, J. S. Sarracino, F. E. Shelley Jr., H. L. Stacey, B. E. Takala, R. T. Thompson, H. E. Tucker, G. J. Yates, H.-J. Ziock, J. D. Zumbro, "An 800-MeV Proton Radiography Facility for Dynamic Experiments," *Nucl. Instr. & Meth*. A424 (1999) pp84-91;

[3] J.A. Cookson, "Radiography with protons", Naturwissenschaften 61, 184-191 (1974)

[4] C. T. Mottershead and J. D. Zumbro, "Magnetic Optics for Proton Radiography", Proceedings of the 1997 Particle Accelerator Conf, Vancouver 1397 (1997)

[5] Rybaryck, L, LANL, Longitudinal Tracking Studies for the AHF booster synchrotron , Proceedings of the 2003 Particle Accelerator Conference (2003) , and Jeffrey Paisner, LANL, private communication